Facile Synthesis and Quantitative Structure–Activity Relationship Study of Antitumor Active 2-(4-Oxo-thiazolidin-2-ylidene)-3-oxo-propionitriles

Mona Maurice Hanna and Riham François George*

Pharmaceutical Chemistry Department, Faculty of Pharmacy, Cairo University; El-Kasr El-Aini Street, Cairo 11562, Egypt. Received June 3, 2012; accepted June 25, 2012

2-(5-Arylidene-4-oxo-3-phenyl-thiazolidin-2-ylidene)-3-oxo-propionitriles 4a–j were prepared *via* condensation of aromatic aldehydes with 4-thiazolidinones 3a, b. The latter was obtained *via* electrophilic attack of phenylisothiocyanate on 3-oxo-propionitriles 1a, b followed by reaction with chloroacetyl chloride under basic condition. Additionally, 2-(5-heteroalicyclic methylene) analogues 5a–h were prepared *via* Mannich reaction of the appropriate secondary amines and formaldehyde with 4-thiazolidinones 3a, b. Many of the synthesized compounds exhibited promising antitumor properties against colon HCT116 and breast T47D cell lines. 3D-Pharmacophore modeling and quantitative structure–activity relationship (QSAR) analysis were combined to explain the observed antitumor properties.

Key words thiazolidinone; quantitative structure–activity relationship; antitumor activity; 3-oxo-propionitrile; HCT116; T47D

Cancer ranks second in diseases leading to mortality, following only cardiovascular diseases. One-quarter of all deaths in the United States are caused by cancer.[1)] Out of the many cancer diseases, breast cancer is the most prevalent cancer in women and represents the second highest leading cause of cancer death in this population after lung cancer.[2)] Colorectal cancer is the third most common cancer in both men and women, 91% of cases are diagnosed in individuals 50 years of age and older.[1)] Chemotherapy is widely used to treat and control cell growth and limit the spread of cancer cells to other sites. Although, there is a success with certain forms of cancer, drug therapy has only limited impact against the three major killers: carcinoma of lung, breast and colorectal system. Therefore, there is a need to develop novel antitumor agents to treat and combat this disease.

Several promising antitumor agents containing thiazolidine and thiazolidinone scaffolds have been identified to have a broad range of anticancer activities.[3–14)] Previously, we reported promising antitumor properties of a variety of 5-arylidene thiazolidinone derivatives **Ia–c** (Fig. 1) exhibiting considerable cytotoxic activity against colon HCT116 cancer cell lines compared with Doxorubicin (reference standard, IC_{50}=0.00686 mM).[15)] In continuation of these previous findings and in order to optimize novel antitumor active agents possessing the same thiazolidinone core, it is intended in the present work to perform some modifications in the adopted structures *via* inserting heteroalicyclic amines (morpholinyl or piperidinyl functions, **4a–j**) instead of the aromatic amines **Ia–c** due to their hydrophilic properties. Moreover, a series of heteroalicyclic methylene containing compounds **5a–h** will be also prepared replacing the arylidene moiety of **Ia–c** (Fig. 1). Additionally, many morpholine and piperidine containing compounds were known as anticancer active agents that exerted their actions *via* inhibition of different targets such as phosphatidylinositol 3-kinases (PI3Ks) and histone deacetylase (HDAC).[16–20)] Moreover, the piperidine derivatives **IIa–e** (Fig. 2) were reported through antitumor activity data obtained by US-NCI to be active against different cell lines exemplified by T47D (breast cancer, GI_{50}=0.00089 mM), HL-60 (TB) (leukemia, GI_{50}=0.00085 mM), SNB-75 (CNS cancer, GI_{50}=0.00185 mM), OVCAR-5 (ovarian cancer, GI_{50}=0.00055 mM), EKVX (non-small lung cell cancer, GI_{50}=0.00202 mM) and PC-3 (prostate cancer, GI_{50}=0.00087 mM).[21)]

Quantitative structure–activity relationship (QSAR) will be also taken into consideration during the present work in order to study the pharmacophoric features of the antitumor active compounds and to determine the parameters controlling the pharmacological properties.

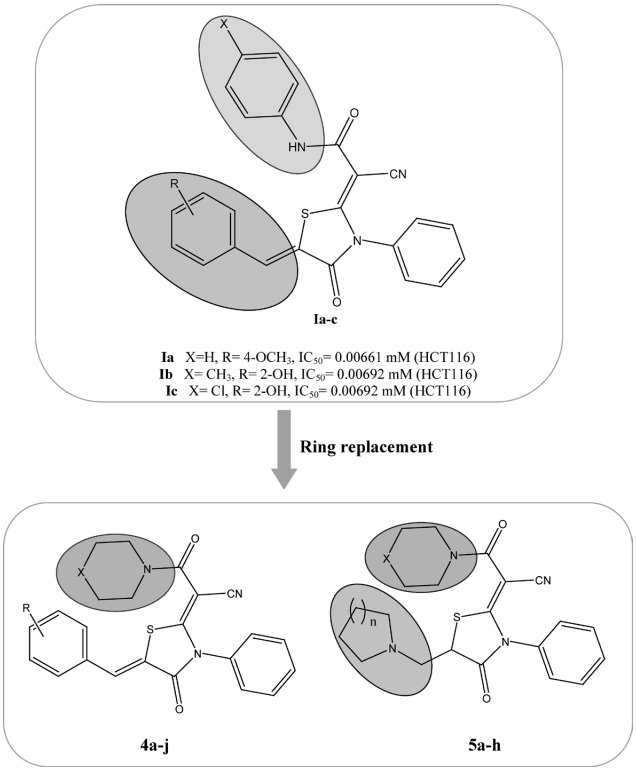

Fig. 1. Reported (**Ia–c**) and Proposed (**4a–j**, **5a–h**) Thiazolidinone Derivatives

The authors declare no conflict of interest.

* To whom correspondence should be addressed. e-mail: rihamfgeorge@yahoo.com

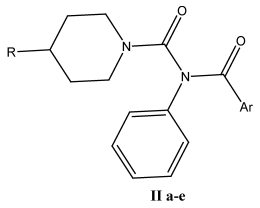

IIa R= H, Ar= $ClC_6H_4OC(CH_3)_2$-, GI_{50}= 0.00089 mM (T47D)
IIb R= C_6H_5, Ar= $ClC_6H_4OC(CH_3)_2$-, GI_{50}= 0.00085 mM (HL-60(TB))
IIc R= C_6H_5, Ar= ClC_6H_4-, GI_{50}= 0.00185 mM (SNB-75), 0.00055 mM (OVCAR-5)
IId R= C_6H_5, Ar= 2-furanyl, GI_{50}=0.00202 mM (EKVX)
IIe R= C_6H_5, Ar= thiphene-2-yl, GI_{50}=0.00087 mM (PC-3)

Fig. 2. Structures of Some Antitumor Active Piperidine Derivatives

Results and Discussion

Chemistry The target 2-(5-arylidene-4-oxo-3-phenyl-thiazolidin-2-ylidene)-3-oxo-propionitriles **4a**–**j** were prepared as depicted in Charts 1 and 2. The starting 3-(morpholin-4-yl)-**1a** and 3-(piperidin-1-yl)-3-oxo-propionitriles **1b** were synthesized according to the previously reported procedures.[22] Electrophilic attack of phenylisothiocyanate on the active methylene of compounds **1a**, **b** in dry tetrahydrofuran (THF) in the presence of potassium hydroxide afforded 3-mercapto-2-carbonyl-3-phenylamino-acrylonitriles **2a**, **b**. The structures of the isolated compounds **2a**, **b** were confirmed by ^{1}H-NMR spectral data, that lacked any signal assigneable for the active methylene function and exhibited signals due to the aromatic ring protons at δ=7.11–7.78, and two exchangeable signals corresponding to NH and SH protons at δ=5.34–5.37 and 10.54–11.08 respectively. Reaction of **2a**, **b** with chloroacetyl chloride in the presence of triethylamine (TEA) in dry THF gave the 4-thiazolidinone derivatives **3a**, **b**. IR spectra of **3a**, **b** revealed two C=O bands at ν=1736–1724 and 1636 cm^{-1} regions. ^{1}H-NMR spectra of **3a**, **b** exhibited the methylene function as a sharp singlet signal at δ=3.90.

The target arylidenes **4a**–**j** were obtained by condensation of the appropriate aromatic aldehydes with **3a**, **b** in dimethylformamide (DMF) in the presence of TEA. The structures of **4a**–**j** were established through different spectroscopic techniques (IR, ^{1}H-NMR, MS) and elemental analyses data. The disappearance of the singlet signal due the methylene protons and the presence of the sharp singlet signal due to the ylidene proton in ^{1}H-NMR spectra added a good confirmation for the assigned structures **4a**–**j**. The appearance of the ylidene proton of compounds **4a**–**c**, **4f**–**h** at δ=7.78–7.86 confirmed the formation of *Z*-isomers.[9,15,23–28] On the other hand, the ylidene proton of compounds **4d** and **4i** were revealed at δ=8.00–8.16, slightly downfield shifted than the other synthesized analogues, which could be attributed to the anisotropic effect of the hydroxyl group oriented at the *o*-position of the arylidene function. Furthermore, reaction of 4-thiazolidinones **3a**, **b** with formaldehyde and the appropriate heteroalicyclic amines

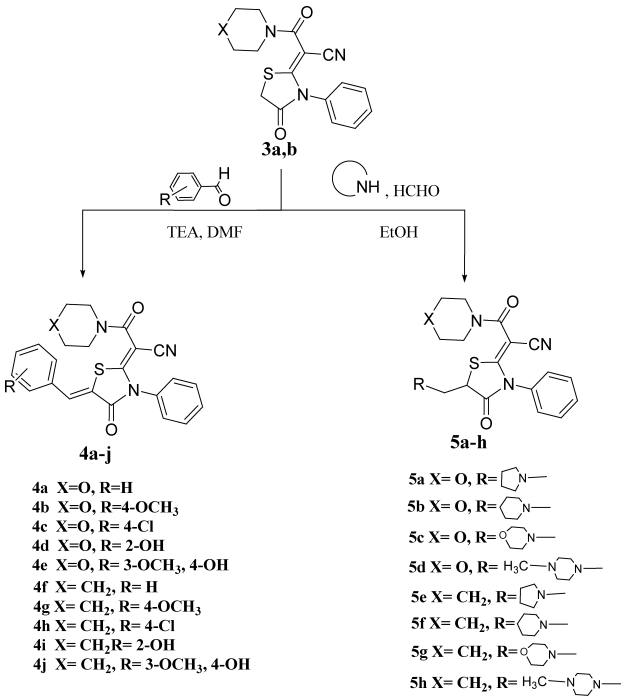

Chart 2. Synthetic Pathway for Preparation of Compounds **4a**–**j** and **5a**–**h**

(pyrrolidine, piperidine, morpholine and *N*-methylpiperazine) through Mannich reaction yielded **5a**–**h**. The structures of the obtained products **5a**–**h** were confirmed by ^{1}H-NMR that revealed the expected heteroalicyclic protons signals in addition to the other skeleton protons (*cf.* Experimental).

Furthermore, reaction of the 3-mercapto-3-phenylamino-acrylonitriles **2a**, **b** with 3-chloropropionyl chloride in THF in the presence of TEA afforded 3-oxo-2-(4-oxo-3-phenyl-[1,3]-thiazinan-2-ylidene)propionitriles **6a**, **b** (Chart 3). Single X-ray crystallography of **6a** (Fig. 3) allowed good confirmation for the assigned structure confirming that the isolated product is *E*-isomer.

Many trials had been performed toward preparation of 2-(5-arylidene-4-oxo-3-phenyl-[1,3]thiazinan-2-ylidene)-3-oxo-propionitriles **7** *via* condensation reaction of different aromatic aldehydes (benzaldehyde, *p*-anisaldehyde, *p*-chlorobenzaldehyde, salicylaldehyde or vanillin) with **6a**, **b** under different reaction conditions. When this reaction was conducted in DMF/TEA, absolute ethanol/piperidine or absolute ethanol/potassium hydroxide at room temperature, or either warming the reaction in DMF/TEA at 60°C, no reaction was occurred. However, upon conducting the reaction at reflux temperature in absolute ethanol/piperidine or absolute ethanol/potassium hydroxide, the hydrolysed products **2a**, **b** were isolated instead of the expected arylidene derivatives **7** (where the structures

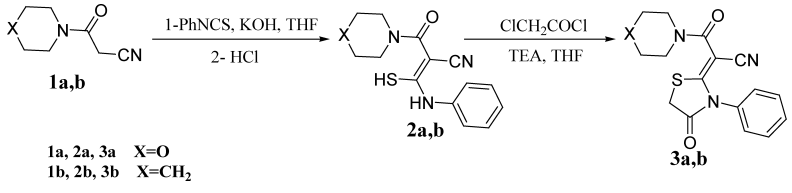

Chart 1. Synthetic Pathway for Preparation of **3a**, **b**

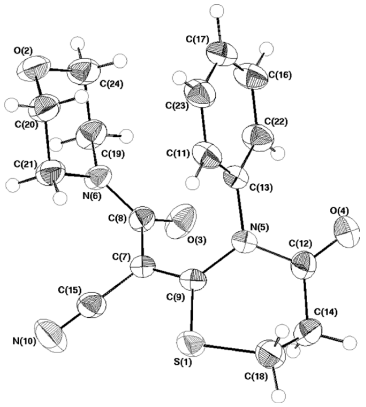

Fig. 3. ORTEP Projection of Single Crystal X-Ray Diffraction of **6a**

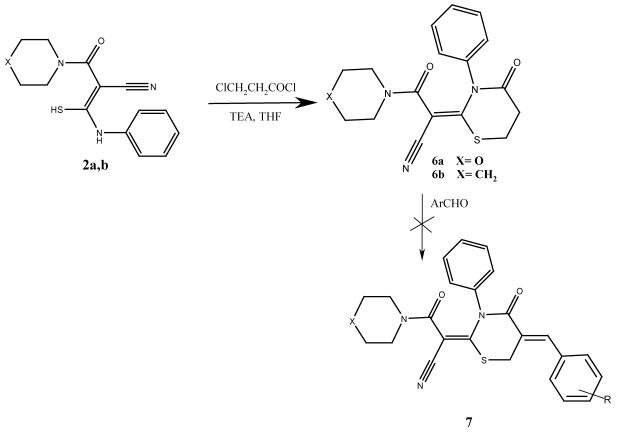

Chart 3. Synthetic Pathway for Preparation of Compounds **6a**, **b**

were established by comparative IR and melting point data). These results could be attributed to the lower activity of the methylene group neighbouring to the cyclic ketonic function of the six membered ring system than the corresponding five membered thiazolidinone system.

Antitumor Activity *In-vitro* antitumor activity of the tested compounds was screened utilizing Sulfo-Rodamine B (SRB) standard method[15,29–35] in the National Cancer Institute, Cairo University, Egypt. All the prepared target compounds (**4a**–**j**, **5a**–**h**) were tested for their antitumor properties against HCT116 "colon" and T47D "breast" cancer cell lines. From the observed antitumor activity data (Table 1), (see also Figs. 1, 2 of the Supplementary data), it has been noticed that the tested compounds showed moderate to potent antitumor activity having IC_{50} values ranging from 0.00586 to 0.04848 mM against HCT116 cancer cell lines and from 0.00646 to 0.05059 mM against T47D cell lines. In most cases, the 5-arylidene derivatives **4a**–**j** exerted promising antitumor activity against both cell lines than the 5-heteroalicyclic methyl analogues **5a**–**h**.

Considering the observed antitumor screening data of the synthesized compounds against HCT116 "colon" cancer cell line, the arylidene piperidine derivatives **4f**–**i** exerted higher potency than the morpholine analogues **4a**–**d**. Compound **4g** was the most effective one with IC_{50}=0.00586 mM compared with Doxorubicin (IC_{50}=0.00686 mM). This derivative was selected by US-NCI for more antitumor activity screening

Table 1. IC_{50} of the Tested Compounds against Human Tumor Cell Lines

Compound	X	R	Tested human tumor cell lines, IC_{50} μg/mL (mM)	
			Colon (HCT 116)	Breast (T47D)
Doxorubicin	—	—	3.73 (0.00686)	7.65 (0.01407)
4a	O	H	3.64 (0.00872)	14.09 (0.03375)
4b	O	4-OCH_3	3.64 (0.00813)	16.25 (0.03631)
4c	O	4-Cl	3.48 (0.0077)	2.92 (0.00646)
4d	O	2-OH	10.91 (0.02517)	3.81 (0.00879)
4e	O	3-OCH_3, 4-OH	12.17 (0.02626)	17.92 (0.03866)
4f	CH_2	H	2.92 (0.00703)	2.86 (0.00688)
4g	CH_2	4-OCH_3	2.61 (0.00586)	3.18 (0.00714)
4h	CH_2	4-Cl	2.92 (0.00649)	3.33 (0.0074)
4i	CH_2	2-OH	3.64 (0.00844)	8.10 (0.01877)
4j	CH_2	3-OCH_3, 4-OH	15.00 (0.0325)	14.50 (0.03142)
5a	O		20.00 (0.04848)	15.45 (0.03754)
5b	O		13.64 (0.03198)	15.91 (0.0373)
5c	O		6.67 (0.01557)	8.10 (0.0189)
5d	O		6.96 (0.01576)	5.83 (0.0132)
5e	CH_2		11.67 (0.02843)	12.11 (0.0295)
5f	CH_2		15.91 (0.03747)	20.95 (0.04934)
5g	CH_2		14.09 (0.03303)	21.58 (0.05059)
5h	CH_2		13.18 (0.02998)	14.21 (0.03233)

utilizing 56 cell lines belonging to nine types of cancers (leukemia, non-small cell lung cancer, colon cancer, CNS cancer, melanoma, ovarian cancer, renal cancer, prostate cancer and breast cancer).[30–35] The observed data expressed as GI_{50} (the concentration resulting in a 50% growth inhibition of the tumor compared with the control experiments), TGI (the concentration resulting in a 100% growth inhibition of the tumor compared with the control experiments) and LC_{50} were presented in Table 2. It showed promising activity against 38 cell lines especially, HOP-92, NCI-H226 (non-small cell lung cancer), GI_{50}=0.000865, 0.00127 mM, respectively, SF-539, SNB-75 (CNS cancer), GI_{50}=0.00144, 0.000811 mM, respectively, MALME-3M, SK-MEL-5 (melanoma), GI_{50}=0.0016, 0.0015 mM, respectively, OVCAR-4, SK-OV-3 (ovarian cancer), GI_{50}=0.00102, 0.00115 mM, respectively, 786-0, A498, RXF 393, UO-31 (renal cancer), GI_{50}=0.00112, 0.00111, 0.00118, 0.00148 mM, respectively and MDA-MB-231/ATCC, HS 578T (breast cancer), GI_{50}=0.00133, 0.00113 mM, respectively.

On the other hand, the antitumor activity of the tested compounds against T47D breast cell lines exhibiting that compound **4c** was the most active with IC_{50} value=0.00646 mM compared with Doxorubicin (IC_{50}=0.01407 mM), the 5-arylidene morpholine derivatives **4c** and **4d** (IC_{50}=0.00646, 0.00879 mM, respectively) were more potent than their piperidine analogues **4h** and **4i** (IC_{50}=0.0074, 0.01877 mM, respectively) (Table 1). However, the piperidine containing compounds **4f** and **4g** exhibited higher antitumor activity (IC_{50}=0.00688, 0.00714 mM, respectively) than the morpholine derivatives **4a** and **4b** (IC_{50}=0.03375, 0.03631 mM, respectively). In addition, compound **5d** showed good activity with IC_{50} values=0.0132 mM.

QSAR Study. 3D-QSAR Pharmacophore Modeling This study was performed using Discovery Studio 2.5 software (Accelrys Inc., San Diego, CA, U.S.A.). A given

Table 2. Antitumor Screening Data of **4g** Expressed in GI_{50}, TGI, LC_{50} Values (mM) Utilizing Human Tumor Cell Lines

Panel/cell lines	GI_{50}	TGI	LC_{50}	Panel/cell lines	GI_{50}	TGI	LC_{50}
Leukemia				Ovarian cancer			
HL-60(TB)	>0.05	>0.05	>0.05	IGROV1	0.00277	>0.05	>0.05
K-562	>0.05	>0.05	>0.05	OVCAR-3	0.00195	>0.05	>0.05
MOLT-4	>0.05	>0.05	>0.05	OVCAR-4	0.00102	ND[a]	>0.05
RPMI-8226	ND[a]	>0.05	>0.05	OVCAR-5	>0.05	>0.05	>0.05
SR	0.0113	>0.05	>0.05	OVCAR-8	0.00167	>0.05	>0.05
Non-small cell lung cancer				NCI/ADR-RES	0.00233	>0.05	>0.05
A549/ATCC	0.00263	>0.05	>0.05	SK-OV-3	0.00115	0.00257	>0.05
EKVX	0.0041	>0.05	>0.05	Renal cancer			
HOP-62	0.00214	0.00938	>0.05	786-0	0.00112	0.0025	>0.05
HOP-92	0.000865	0.00286	>0.05	A498	0.00111	0.00496	>0.05
NCI-H226	0.00127	>0.05	>0.05	ACHN	0.00247	0.0135	>0.05
NCI-H23	0.00771	>0.05	>0.05	CAKI-1	>0.05	>0.05	>0.05
NCI-H460	0.00308	>0.05	>0.05	RXF 393	0.00118	0.00357	0.0325
NCI-H522	>0.05	>0.05	>0.05	SN12C	0.00225	>0.05	>0.05
Colon cancer				TK-10	0.00371	>0.05	>0.05
COLO 205	>0.05	>0.05	>0.05	UO-31	0.00148	>0.05	>0.05
HCC-2998	>0.05	>0.05	>0.05	Prostate cancer			
HCT-15	>0.05	>0.05	>0.05	PC-3	ND[a]	>0.05	>0.05
HT29	>0.05	>0.05	>0.05	DU-145	>0.05	>0.05	>0.05
KM12	>0.05	>0.05	>0.05	Breast cancer			
SW-620	>0.05	>0.05	>0.05	MCF7	>0.05	>0.05	>0.05
CNS cancer				MDA-MB-231/ ATCC	0.00133	0.00434	>0.05
SF-268	0.00374	>0.05	>0.05	HS 578T	0.00113	0.00379	>0.05
SF-295	0.00776	>0.05	>0.05	BT-549	0.0223	>0.05	>0.05
SF-539	0.00144	ND[a]	>0.05	MDA-MB-468	0.00343	>0.05	>0.05
SNB-19	0.00409	>0.05	>0.05				
SNB-75	0.000811	0.00214	0.0105				
U251	0.00297	>0.05	>0.05				
Melanoma							
LOX IMVI	0.00257	>0.05	>0.05				
MALME-3M	0.0016	>0.05	>0.05				
M14	0.00417	>0.05	>0.05				
MDA-MB-435	>0.05	>0.05	>0.05				
SK-MEL-2	0.00405	0.0412	>0.05				
SK-MEL-28	0.00241	>0.05	>0.05				
SK-MEL-5	0.0015	>0.05	>0.05				
UACC-257	>0.05	>0.05	>0.05				
UACC-62	0.00211	>0.05	>0.05				

a) ND=not determined.

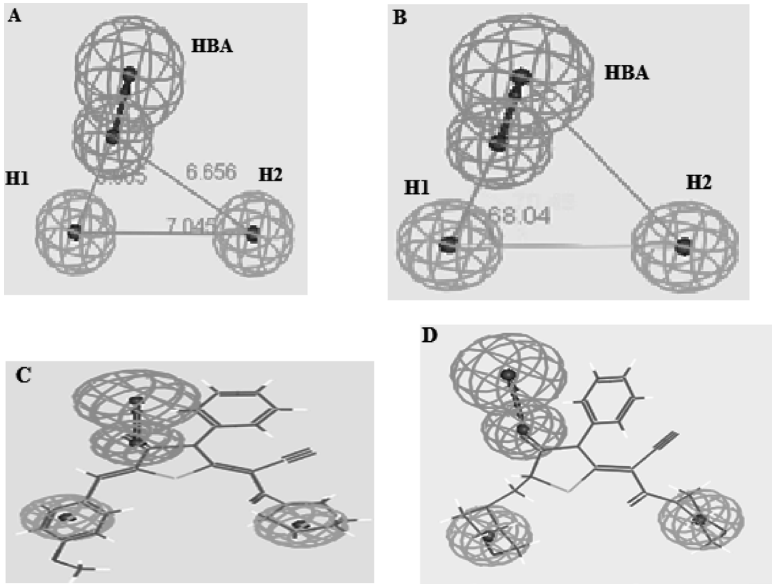

Fig. 4. (A) Constraint Distances (Å) and (B) Constraint Angels (°) between Features of the Generated Pharmacophore, (C) Mapping of **4g** in the Generated Pharmacophore, (D) Mapping of **5c** in the Generated Pharmacophore

Table 3. Constraint Distances (Å) and Angles (°) between Features of the Generated Pharmacophore for Colon HCT116 Cancer Cell Lines

Constraint distances (Å)	Constraint angles (°)
(HBA)–(H1)=3.905; (HBA)–(H2)=6.656; (H2)–(H1)=7.045 Å	(H2)–(H1)–(HBA)=68.04°; (H2)–(HBA)–(HBA vector)=55.16°; (HBA vector)–(H2)–(H1)=70.48°

hypothesis could be combined with a known activity data to create a 3D-QSAR model that identifies overall aspects of molecular structure governing activity. 3D-QSAR based on pharmacophore was constructed using collections of molecules with activities ranging over a number of orders of magnitude. Pharmacophores explain the variability of bioactivity with respect to the geometric localization of the chemical features present in the molecules.[15,35)]

Twenty nine compounds (**4a**–**f**, **4h**–**j**, **5a**, **b**, **5d**–**h** and the previously prepared **Ia**–**j** and **IIIa**–**c**[15)]) were taken as a training set and the remaining two compounds, **4g** (with potent antitumor activity) and **5c** (with mild activity) were used as a test set. The observed HYPOGEN identifies a 3D array of a maximum of three chemical features common to the training set that provide relative alignment for each input molecule, consistent with its binding mode to a proposed common receptor site. The chemical features considered were: two hydrophobic sites (H1, H2) and one hydrogen bond acceptors (HBA) (Figs. 4A, B, Table 3 exhibit constraint distances and angles between features of the generated pharmacophore). Through the pharmacophore mapping study, it was found that the major structural factors affecting the potency of these compounds were related to their basic skeleton. The controlling features were two hydrophobic sites represented by the arylidene and morpholine or piperidine moieties together with a hydrogen bond acceptor of the amide carbonyl group for **4a**–**j**. While compounds **5a**–**h** had not been fitted well to the generated pharmacophore as they lacked the arylidene moiety, therefore, their fit values were smaller than those of **4a**–**j** that explained their mild antitumor activity (Table 4).

QSAR Modeling Despite of the significance of pharmacophoric hypotheses for understanding ligand molecule affinity and 3D search queries, their predictive value as 3D-QSAR models is generally limited by steric shielding and bioactivity-modulating auxiliary groups (electron donating or withdrawing functionalities).[15,35–38)] Thus, a classical QSAR analysis was employed to search for the best combination of orthogonal pharmacophores using a fit value and other structural descriptors (connectivity, topological, *etc.*) capable of explaining bioactivity variation across a collected list of the descriptors, allowing different pharmacophoric models competing within the 3D-QSAR framework.

A set of 29 compounds (**4a**–**f**, **4h**–**j**, **5a**, **b**, **5d**–**h** and the previously reported **Ia**–**j** and **IIIa**–**c**[15)]) was used as a training set for a QSAR modeling. The remaining 2 compounds (**4g** and **5c**) were adopted as an external test subset for validating the QSAR model. Many molecular descriptors were calculated for each compound employing a calculated molecular properties module. The calculated descriptors including various simple and valence connectivity indices, electro-topological state indices, single point quantum-mechanical descriptors (*via* the AM1 model) and other molecular descriptors, were considered. Furthermore, the training set compounds were fitted against the corresponding pharmacophore hypotheses generated by the HYPOGEN automatic runs and their fit values (produced by the best-fit command) were added as additional molecular descriptors. Genetic function approximation (GFA) was employed to search for the best possible QSAR regression equation capable of correlating the variations in biological activities of the training set compounds with variations in the generated descriptors, *i.e.* multiple linear regression modeling (MLR).[15,35,39)] Equation 1 shows our best-performing QSAR model (Fig. 5 exhibits the corresponding scatter plots of experimental *versus* estimated bioactivity values for the

Table 4. Best Fit Values and Estimated Activities for 29 Compounds of the Training Set Mapped with the Generated 3D-Pharmacophore Model

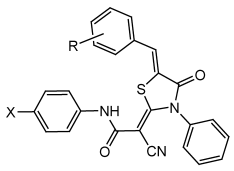

Ia-j

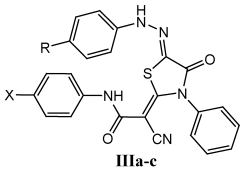

IIIa-c

Compound	X	R	Observed activity	Estimated activity	Fit value
4a	O	H	8.72×10^{-3}	18.04×10^{-3}	5.86
4b	O	4-OCH_3	8.13×10^{-3}	10.91×10^{-3}	5.92
4c	O	4-Cl	7.7×10^{-3}	10.80×10^{-3}	6.05
4d	O	2-OH	25.17×10^{-3}	11.65×10^{-3}	5.88
4e	O	3-OCH_3, 4-OH	26.26×10^{-3}	11.64×10^{-3}	5.93
4f	CH_2	H	7.03×10^{-3}	10.74×10^{-3}	6.08
4h	CH_2	4-Cl	6.49×10^{-3}	10.22×10^{-3}	6.08
4i	CH_2	2-OH	8.44×10^{-3}	11.41×10^{-3}	6.04
4j	CH_2	3-OCH_3, 4-OH	32.5×10^{-3}	11.41×10^{-3}	5.48
5a	O		48.48×10^{-3}	35.16×10^{-3}	5.74
5b	O		31.98×10^{-3}	38.58×10^{-3}	5.75
5d	O	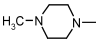	15.76×10^{-3}	32.54×10^{-3}	5.69
5e	CH_2		28.43×10^{-3}	39.23×10^{-3}	5.51
5f	CH_2		37.47×10^{-3}	38.17×10^{-3}	5.78
5g	CH_2		33.03×10^{-3}	23.29×10^{-3}	5.74
5h	CH_2	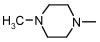	29.98×10^{-3}	30.46×10^{-3}	5.89
Ia	H	4-OCH_3	6.61×10^{-3}	10.57×10^{-3}	6.09
Ib	CH_3	2-OH	6.92×10^{-3}	8.88×10^{-3}	6.16
Ic	Cl	2-OH	6.92×10^{-3}	7.93×10^{-3}	6.21
Id	H	2-OH	7.80×10^{-3}	12.84×10^{-3}	6.00
Ie	Cl	4-Cl	9.15×10^{-3}	16.33×10^{-3}	5.90
If	CH_3	4-OCH_3	9.95×10^{-3}	14.15×10^{-3}	5.96
Ig	CH_3	H	10.97×10^{-3}	12.99×10^{-3}	6.00
Ih	CH_3	4-Cl	28.39×10^{-3}	16.01×10^{-3}	5.91
Ii	H	H	33.29×10^{-3}	16.59×10^{-3}	5.89
Ij	Cl	H	38.87×10^{-3}	8.06×10^{-3}	6.21
IIIa	CH_3	Cl	14.86×10^{-3}	27.45×10^{-3}	5.67
IIIb	H	OCH_3	46.35×10^{-3}	44.07×10^{-3}	5.47
IIIc	H	H	113.77×10^{-3}	72.71×10^{-3}	5.25

training set compounds against HCT116 tumor cell lines). The goodness of the model was validated by squared correlation coefficient (R^2) and residuals between the predicted and experimental activity of the training set (Table 5).

Potency (IC_{50}) against HCT116 (colon cancer) cell line (N "number of molecules in the training set"=29, R^2 "squared correlation coefficient value"=0.726)

$$IC_{50} = 604.41 - 0.298\times[\text{Molecular\_SurfaceArea}] - 398.59\times[\text{Jurs\_RNCG}] - 67.65\times[\text{FitValue}] \quad (1)$$

Where the Jurs_RNCG is a relative negative charge descriptor that described the charge of most negative atom divided by total negative charge.

Searching for set descriptors (D), containing D descriptors of optimal subset (d), where $d \ll D$ ones with minimum standard deviation (S), by means of multivariable linear regression (MLR) technique.

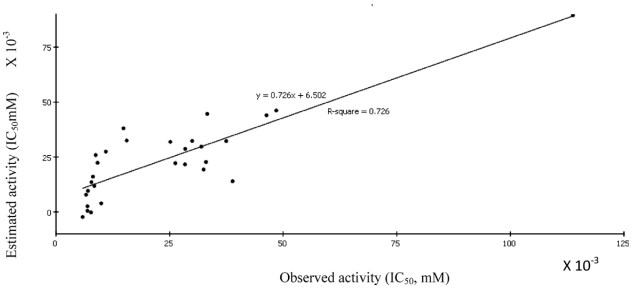

Fig. 5. Estimated Activity *versus* Observed Activity (IC_{50}) of the Tested Compounds against HCT116 (Colon) Human Tumor Cell Line

Table 5. Estimated Activity Data of the Training Set against HCT116 (Colon Cancer) Cell Line and Calculated Descriptors Governing Activity According to Eq. 1

Compound	Mol. surface area	Jurs_RNCG	Fit value	Observed activity	Estimated activity	Residual
4a	391.60	0.163	5.86	8.72×10^{-3}	26.27×10^{-3}	-17.55×10^{-3}
4b	424.15	0.149	5.92	8.13×10^{-3}	17.88×10^{-3}	-9.75×10^{-3}
4c	414.67	0.165	6.05	7.7×10^{-3}	5.93×10^{-3}	1.77×10^{-3}
4d	404.88	0.148	5.88	25.17×10^{-3}	26.88×10^{-3}	-1.71×10^{-3}
4e	437.43	0.134	5.93	26.26×10^{-3}	19.14×10^{-3}	7.12×10^{-3}
4f	392.95	0.144	6.08	7.03×10^{-3}	18.14×10^{-3}	-11.11×10^{-3}
4h	416.03	0.145	6.08	6.49×10^{-3}	11.10×10^{-3}	-4.61×10^{-3}
4i	406.23	0.156	6.04	8.44×10^{-3}	9.28×10^{-3}	-0.84×10^{-3}
4j	438.78	0.139	5.48	32.5×10^{-3}	9.25×10^{-3}	23.25×10^{-3}
5a	392.02	0.186	5.74	48.48×10^{-3}	42.31×10^{-3}	6.17×10^{-3}
5b	407.99	0.181	5.75	31.98×10^{-3}	21.76×10^{-3}	10.22×10^{-3}
5d	429.29	0.165	5.69	15.76×10^{-3}	21.48×10^{-3}	-5.72×10^{-3}
5e	393.37	0.167	5.51	28.43×10^{-3}	35.41×10^{-3}	-6.98×10^{-3}
5f	409.34	0.162	5.78	37.47×10^{-3}	44.57×10^{-3}	-7.10×10^{-3}
5g	407.99	0.176	5.74	33.03×10^{-3}	21.20×10^{-3}	11.83×10^{-3}
5h	430.64	0.145	5.89	29.98×10^{-3}	29.57×10^{-3}	0.41×10^{-3}
Ia	425.47	0.145	6.09	6.61×10^{-3}	7.76×10^{-3}	-1.15×10^{-3}
Ib	425.61	0.147	6.16	6.92×10^{-3}	1.85×10^{-3}	5.07×10^{-3}
Ic	429.27	0.149	6.21	6.92×10^{-3}	-3.51×10^{-3}	10.43×10^{-3}
Id	406.20	0.148	6.00	7.80×10^{-3}	17.96×10^{-3}	-10.16×10^{-3}
Ie	439.06	0.130	5.90	9.15×10^{-3}	22.29×10^{-3}	-13.14×10^{-3}
If	444.88	0.144	5.96	9.95×10^{-3}	11.05×10^{-3}	-1.10×10^{-3}
Ig	412.34	0.127	6.00	10.97×10^{-3}	24.94×10^{-3}	-13.97×10^{-3}
Ih	435.41	0.128	5.91	28.39×10^{-3}	23.77×10^{-3}	4.62×10^{-3}
Ii	392.92	0.128	5.89	33.29×10^{-3}	37.42×10^{-3}	-4.13×10^{-3}
Ij	415.99	0.129	6.21	38.87×10^{-3}	8.89×10^{-3}	29.98×10^{-3}
IIIa	446.85	0.115	5.67	14.86×10^{-3}	41.48×10^{-3}	-26.62×10^{-3}
IIIb	436.91	0.131	5.47	46.35×10^{-3}	51.81×10^{-3}	-5.46×10^{-3}
IIIc	404.37	0.115	5.25	113.77×10^{-3}	82.72×10^{-3}	31.05×10^{-3}

Table 6. External Validation for the Established QSAR Models Utilizing Promising **4g** and **5c** Mild Antitumor Active Agents

Cell lines	Compound	3D-QSAR pharmacophore			Classical QSAR	
		Experimental activity (IC_{50})	Predicted activity (IC_{50})	Fit value	Experimental activity (IC_{50})	Predicted activity (IC_{50})
HCT116	**4g**	5.86×10^{-3}	7.65×10^{-3}	5.31	5.86×10^{-3}	6.76×10^{-3}
	5c	15.57×10^{-3}	22.14×10^{-3}	5.04	15.57×10^{-3}	13.13×10^{-3}

$$S = \frac{1}{(N-d-1)}\sum_{i=1}^{N}\text{resi}$$

$$\text{FIT} = \frac{R(d)^2(N-d-1)}{(N+d^2)(1-R^2)}$$

Where; N, is the number of molecules of the training set; resi, is the residual for molecule; i, is the difference between the experimental property (p) and predicted property (ppred). More precisely, the Kubinyi function (FIT)[15,35] is a statistical parameter which is closely related to the Fisher ratio (F), but avoids the main disadvantage of the latter of being too sensitive to changes in small d values, and poorly sensitive to changes in large d values. The FIT (d) criterion has a low sensitivity to changes in small d values and a substantially increasing sensitivity for large d values. The greater the FIT value the better the linear equation.[15,35,40] It is given by the following equation, "where $R(d)$ is the correlation coefficient for a model with (d) descriptors." The observed FIT value is 2.91 corresponding to model due to HCT116 cancer cell lines. Where N=29, R=0.852, S=0.544, FIT=2.91.

Validation of QSAR External validation of the determined QSAR equations was performed utilizing two of our synthesized analogues exhibiting promising (**4g**) and mild (**5c**). The observed activities and those provided by QSAR study are presented in Table 6.

Conclusion

3-Oxo-2-(4-oxo-3-phenyl-thiazolidin-2-ylidene)propionitriles **3a**,**b** were synthesized *via* reaction of 3-mercapto-3-oxo-3-phenylamino-acrylonitriles **2a**,**b** with chloroacetyl chloride in the presence of TEA. Reaction of **3a**,**b** with either aromatic aldehydes or heteroalicyclic secondary amines and formaldehyde afforded 2-(5-arylidene-4-oxo-3-phenyl-thiazolidin-2-ylidene)-2-cyano-3-oxo-propionitriles **4a**–**j** and 2-(5-heteroalicyclic methyl) analogues **5a**–**h**, respectively.

Furthermore, (2*E*) 3-oxo-2-(4-oxo-3-phenyl-[1,3]thiazinan-2-ylidene)-propionitriles **6a**,**b** were prepared stereoselectively *via* reaction of **2a**,**b** with 3-chloropropionyl chloride in the presence of TEA. Many trials to obtain the arylidene derivatives **7** *via* condensation of different aromatic aldehydes with **6a**,**b** were unsuccessful.

The synthesized **4a**–**j** and **5a**–**h** were tested for their anticancer activity against colon (HCT116) and breast (T47D) cancer cell lines. It was concluded that the 5-arylidene moiety is essential for the antitumor activity, and in most cases, the piperidine derivatives exhibited better activity than morpholine analogues. Compound **4g** was the most active compound against colon HCT116 with $IC_{50}=0.00586$ mM compared with Doxorubicin ($IC_{50}=0.00686$ mM) and **4c** had the highest activity against breast T47D with $IC_{50}=0.00646$ mM compared with Doxorubicin ($IC_{50}=0.01407$ mM). QSAR study confirmed the obtained antitumor results, where the three pharmacophoric features for HCT116 activity were two hydrophobic sites and a hydrogen bond acceptor. Classical QSAR studies of HCT116 (colon) cancer cell lines delivered Eq. 1 of three descriptors with $R^2=0.726$. The most important descriptor in the equation was the fit value derived from mapping of the synthesized analogues into the generated pharmacophore. The other controlling descriptors were the molecular surface area and Jurs_RNCG.

External validation of the established QSAR models utilizing two of our synthesized analogues exhibiting promising (**4g**) and mild (**5c**) antitumor properties, revealed good agreement between the experimental and the calculated data. It can be concluded that combination of 3D-pharmacophore modeling and QSAR provides an effective technique for understanding the observed pharmacological properties and thus could be adopted for developing effective lead structures.

Experimental

Chemistry Melting points were measured with an Electrothermal Stuart SMP_3 digital melting point apparatus. IR spectra (KBr disc) were recorded on Shimadzu FT-IR 8400S infrared spectrophotometer. NMR spectra were recorded on a Varian Mercury VX 300 spectrometer (^{1}H: 300, ^{13}C: 75 MHz) using TMS as an internal standard and on JOEL (Eclipse) 400 (^{1}H: 400, ^{13}C: 100 MHz). Mass spectra were measured on a Shimadzu GCMS-QP2010 Plus spectrometer (EI, 70 eV). Elemental analyses were carried out at the Microanalytical center, Faculty of Science, Cairo University, Egypt, and at the Regional center for mycology and biotechnology, Al-Azhar University, Egypt. Reagents and solvents used in synthesis were purchased from Sigma-Aldrich. Compounds **1a**,**b** were prepared according to the reported procedures.[22]

General Procedure for Preparation of (2a,b) To an ice cold mixture of **1a**,**b** (5 mmol) and fine powdered potassium hydroxide (0.28 g, 5 mmol) in dry THF (25 mL) was added dropwise a solution of phenylisothiocyanate (0.68 g, 0.61 mL, 5 mmol) in dry THF (10 mL). The mixture was stirred at room temperature for 48 h, and it was poured on water (200 mL) with stirring. The obtained solution was neutralized with dilute HCl and the obtained precipitate was filtered, washed with water and crystallized from ethanol to obtain **2a**,**b** in a pure form.

3-Mercapto-2-(morpholine-4-carbonyl)-3-phenylamino-acrylonitrile (**2a**): Yellow crystals, 61% yield, mp 122–124°C. ^{1}H-NMR ($CDCl_3$, 300 MHz) δ: 3.45–3.82 (8H, m, morpholine protons), 5.37 (1H, s, NH exch. D_2O), 7.11–7.77 (5H, m, aromatic H), 11.08 (1H, s, SH exch. D_2O). IR (KBr) cm^{-1}: 3271 (NH), 3050–3010 (aromatic CH), 2967–2859 (aliphatic CH), 2172 (C≡N), 1650 (C=O), 1632 (bending NH), 1593–1535 (C=C). *Anal.* Calcd for $C_{14}H_{15}N_3O_2S$ (289.36): C, 58.11; H, 5.23; N, 14.52. Found: C, 57.90; H, 5.30; N, 14.51.

3-Mercapto-3-phenylamino-2-(piperidine-1-carbonyl)-acrylonitrile (**2b**)[41]: Yellow crystals, 75% yield, mp 160–162°C. ^{1}H-NMR ($CDCl_3$, 300 MHz) δ: 1.61–1.74 (6H, m, piperidine protons), 3.57–3.76 (4H, m, $(CH_2)_2N$ piperidine protons), 5.34 (1H, s, NH exch. D_2O), 7.24–7.78 (m, 5H, aromatic H), 10.54 (1H, s, SH exch. D_2O). IR (KBr) cm^{-1}: 3237 (NH), 3063–3017 (aromatic CH), 2990–2862 (aliphatic CH), 2172 (C≡N), 1650 (C=O), 1632 (bending NH), 1593–1535 (C=C). *Anal.* Calcd for $C_{15}H_{17}N_3OS$ (287.39): C, 62.69; H, 5.96; N, 14.62. Found: C, 62.83; H, 6.11; N, 15.08.

General Procedure for the Preparation of (3a,b) A solution of **2a**,**b** (3 mmol) and TEA (0.61 g, 0.84 mL, 6 mmol) in dry THF (15 mL) was cooled to −5°C in an ice/salt bath and a solution of chloroacetyl chloride (0.34 g, 0.24 mL, 3 mmol) in dry THF (5 mL) was added dropwise. The mixture was stirred overnight at room temperature, and the formed precipitate was filtered and dried. The residue was suspended in water, stirred for 5 min, and filtered. The crude product was crystallized from ethanol.

3-Morpholin-4-yl-3-oxo-2-(4-oxo-3-phenyl-thiazolidin-2-ylidene)propionitrile (**3a**): White crystals, 80% yield, mp 188–190°C. ^{1}H-NMR ($CDCl_3$, 300 MHz) δ: 3.56 (4H, t, J=4.2 Hz, $(CH_2)_2N$ morpholine protons), 3.67 (4H, t, J=4.2 Hz, $(CH_2)_2O$ morpholine protons), 3.90 (2H, s, CH_2), 7.28–7.59 (5H, m, aromatic H). IR (KBr) cm^{-1}: 3059 (aromatic CH), 2974–2855 (aliphatic CH), 2199 (C≡N), 1736 (C=O thiazolidinone), 1636 (C=O), 1551–1512 (C=C). *Anal.* Calcd for $C_{16}H_{15}N_3O_3S$ (329.38): C, 58.35; H, 4.59; N, 12.76. Found: C, 58.13; H, 4.69; N, 12.93.

3-Oxo-2-(4-oxo-3-phenyl-thiazolidin-2-ylidene)-3-piperidin-1-yl-propionitrile (**3b**): White crystals, 86% yield, mp 216–218°C. ^{1}H-NMR ($CDCl_3$, 300 MHz) δ: 1.55–1.62 (6H, m, piperidine protons), 3.49–3.51 (4H, m, $(CH_2)_2N$ piperidine protons), 3.90 (2H, s, CH_2), 7.26–7.61 (5H, m, aromatic H). IR (KBr) cm^{-1}: 3050 (aromatic CH), 2993–2855 (aliphatic CH), 2191 (C≡N), 1724 (C=O thiazolidinone), 1636 (C=O), 1558-1497 (C=C). *Anal.* Calcd for $C_{17}H_{17}N_3O_2S$ (327.41): C, 62.37; H, 5.23; N, 12.83. Found: C, 62.49; H, 5.19; N, 13.14.

General Procedure for the Preparation of (4a–j) A solution of **3a**,**b** (1 mmol), the appropriate aldehyde (1 mmol) and TEA (0.10 g, 0.14 mL, 1 mmol) in DMF (5 mL) was stirred at 70°C for 6 h. The mixture was cooled and the obtained precipitate was filtered, washed and crystallized from ethanol.

2-(5-Benzylidene-4-oxo-3-phenyl-thiazolidin-2-ylidene)-3-morpholin-4-yl-3-oxo-propionitrile (**4a**): Yellow crystals, 30% yield, mp 310–312°C (dec.). ^{1}H-NMR ($CDCl_3$, 300 MHz) δ: 3.61 (4H, t, J= 4.2 Hz, $(CH_2)_2N$ morpholine protons), 3.71 (4H, t, J=4.2 Hz, $(CH_2)_2O$ morpholine protons), 7.27–7.66 (10H, m, aromatic H), 7.86 (1H, s, =CH). ^{13}C-NMR (DMSO-d_6, 75 MHz) δ: 43.8 [$(CH_2)_2N$ of morpholine], 66.1 [$(CH_2)_2O$ of morpholine], 77.8 (C=C–CN), 112.0 (CN), 118.0, 122.1, 122.8, 124.6, 125.8, 127.6 (aromatic carbons), 129.4 (C of thiazolidinone attached to olefinic CH), 130.5 (aromatic C attached to N of the 4-thiazolidinone ring), 132.1 (C=CH), 133.9 (aromatic C

attached to olefinic CH), 161.7 (C=O of thiazolidinone), 162.2 (C=O), 166.3 (C=C–CN). IR (KBr) cm^{-1}: 3050–3028 (aromatic CH), 2967–2859 (aliphatic CH), 2191 (C≡N), 1717 (C=O thiazolidinone), 1647 (C=O), 1547–1493 (C=C). *Anal.* Calcd for $C_{23}H_{19}N_3O_3S$ (417.49): C, 66.17; H, 4.59; N, 10.06. Found: C, 66.33; H, 4.62; N, 10.32.

2-[5-(4-Methoxybenzylidene)-4-oxo-3-phenyl-thiazolidin-2-ylidene]-3-morpholin-4-yl-3-oxo-propionitrile (**4b**): Yellow crystals, 35% yield, mp 295–297°C (dec.). ^{1}H-NMR ($CDCl_3$, 300 MHz) δ: 3.59–3.61 (4H, m, $(CH_2)_2$N morpholine protons), 3.69–3.71 (4H, m, $(CH_2)_2$O morpholine protons), 3.90 (3H, s, OCH_3), 7.02 (2H, d, J=8.7 Hz, protons o-OCH_3), 7.35–7.63 (7H, m, aromatic H), 7.81 (1H, s, =CH). ^{13}C-NMR (DMSO-d_6, 100 MHz) δ: 45.3 [$(CH_2)_2$N of morpholine], 55.5 (OCH_3), 66.0 [$(CH_2)_2$O of morpholine], 69.7 (C=C–CN), 115.1 (CN), 119.7, 120.0, 121.9, 122.5, 123.6, 124.7 (aromatic carbons), 126.9 (aromatic C attached to olefinic CH), 129.4 (C of thiazolidinone attached to olefinic CH), 132.4 (aromatic C attached to N of the 4-thiazolidinone ring), 134.9 (C=CH), 153.1 (aromatic C attached to OCH_3 group), 162.2 (C=O of thiazolidinone), 163.0 (C=O), 166.1 (C=C–CN). IR (KBr) cm^{-1}: 3065–3020 (aromatic CH), 2965–2865 (aliphatic CH), 2191 (C≡N), 1713 (C=O thiazolidinone), 1655 (C=O), 1589–1508 (C=C). MS m/z: 448.35 (M^+), 449.30 (M^++1), 450.30 (M^++2), 361, 334.20, 164.10, 77.10. *Anal.* Calcd for $C_{24}H_{21}N_3O_4S$ (447.52): C, 64.41; H, 4.73; N, 9.39. Found: C, 64.59; H, 4.80; N, 9.56.

2-[5-(4-Chlorobenzylidene)-4-oxo-3-phenyl-thiazolidin-2-ylidene]-3-morpholin-4-yl-3-oxo-propionitrile (**4c**): Yellow crystals, 32% yield, mp 334–336°C (dec.). ^{1}H-NMR ($CDCl_3$, 300 MHz) δ: 3.61 (4H, t, J=4.2 Hz, $(CH_2)_2$N morpholine protons), 3.71 (4H, t, J=4.2 Hz, $(CH_2)_2$O morpholine protons), 7.35–7.63 (9H, m, aromatic H), 7.79 (1H, s, =CH). IR (KBr) cm^{-1}: 3051 (aromatic CH), 2982–2855 (aliphatic CH), 2191 (C≡N), 1701 (C=O thiazolidinone), 1647 (C=O), 1593–1543 (C=C). MS m/z: 451.30 (M^+), 452.30 (M^++1), 453.30 (M^++2), 365.20 (42.93), 367.20 (13.38), 168.05 (41.75), 170.05 (18.77), 77.10 (100). *Anal.* Calcd for $C_{23}H_{18}ClN_3O_3S$ (451.94): C, 61.13; H, 4.01; N, 9.30. Found: C, 61.41; H, 4.13; N, 9.68.

2-[5-(2-Hydroxybenzylidene)-4-oxo-3-phenyl-thiazolidin-2-ylidene]-3-morpholin-4-yl-3-oxo-propionitrile (**4d**): Orange crystals, 30% yield, mp 248–250°C (dec.). ^{1}H-NMR (DMSO-d_6, 300 MHz) δ: 3.48–3.57 (8H, m, morpholine protons), 6.99–7.55 (9H, m, aromatic H), 8.00 (1H, s, =CH), 10.62 (1H, s, OH exch. D_2O). ^{13}C-NMR (DMSO-d_6, 75 MHz) δ: 46.8 [$(CH_2)_2$N of morpholine], 66.0 [$(CH_2)_2$O of morpholine], 78.0 (C=C–CN), 112.8 (CN), 116.2 (aromatic C attached to olefinic CH), 118.7, 119.8, 120.2, 120.9, 127.8, 128.9, 129.0 (aromatic carbons), 130.4 (C of thiazolidinone attached to olefinic CH), 132.4 (aromatic C attached to N of the 4-thiazolidinone ring), 134.8 (C=CH), 157.2 (aromatic C attached to OH), 159.8 (C=O of thiazolidinone), 162.2 (C=O), 166.1 (C=C–CN). IR (KBr) cm^{-1}: 3445 (OH), 3028 (aromatic CH), 2965–2865 (aliphatic CH), 2195 (C≡N), 1713 (C=O thiazolidinone), 1636 (C=O), 1585–1520 (C=C). *Anal.* Calcd for $C_{23}H_{19}N_3O_4S$ (433.49): C, 63.73; H, 4.42; N, 9.69. Found: C, 63.89; H, 4.36; N, 9.97.

2-[5-(4-Hydroxy-3-methoxy-benzylidene)-4-oxo-3-phenyl-thiazolidin-2-ylidene]-3-morpholin-4-yl-3-oxo-propionitrile (**4e**): Yellow crystals, 30% yield, mp 248–250°C (dec.). ^{1}H-NMR ($CDCl_3$, 300 MHz) δ: 3.60 (4H, t, J=4.5 Hz, $(CH_2)_2$N morpholine protons), 3.71 (4H, t, J=4.5 Hz, $(CH_2)_2$O morpholine protons), 4.00 (3H, s, OCH_3), 7.03–7.62 (8H, m, aromatic H), 7.78 (1H, s, OH exch. D_2O), 8.03 (1H, s, =CH). IR (KBr) cm^{-1}: 3291 (OH), 3067–3021 (aromatic CH), 2963–2855 (aliphatic CH), 2195 (C≡N), 1709 (C=O thiazolidinone), 1663 (C=O), 1620–1516 (C=C). *Anal.* Calcd for $C_{24}H_{21}N_3O_5S$ (463.52): C, 62.19; H, 4.57; N, 9.07. Found: C, 62.42; H, 4.69; N, 9.31.

2-(5-Benzylidene-4-oxo-3-phenyl-thiazolidin-2-ylidene)-3-oxo-3-piperidin-1-yl-propionitrile (**4f**): Yellow crystals, 40% yield, mp 272–274°C (dec.). ^{1}H-NMR ($CDCl_3$, 300 MHz) δ: 1.64 (6H, brs, piperidine protons), 3.55 (4H, brs, $(CH_2)_2$N piperidine protons), 7.36–7.65 (10H, m, aromatic H), 7.83 (1H, s, =CH). IR (KBr) cm^{-1}: 3040–3028 (aromatic CH), 2932–2847 (aliphatic CH), 2195 (C≡N), 1717 (C=O thiazolidinone), 1655 (C=O), 1597–1493 (C=C). *Anal.* Calcd for $C_{24}H_{21}N_3O_2S$ (415.52): C, 69.38; H, 5.09; N, 10.11. Found: C, 69.48; H, 5.18; N, 10.43.

2-[5-(4-Methoxybenzylidene)-4-oxo-3-phenyl-thiazolidin-2-ylidene]-3-oxo-3-piperidin-1-yl-propionitrile (**4g**): Yellow crystals, 45% yield, mp 268–270°C (dec.). ^{1}H-NMR ($CDCl_3$, 300 MHz) δ: 1.64 (6H, brs, piperidine protons), 3.55 (4H, brs, $(CH_2)_2$N piperidine protons), 3.89 (3H, s, OCH_3), 7.01 (2H, d, J=8.7 Hz, o-OCH_3), 7.35–7.62 (7H, m, aromatic H), 7.78 (1H, s, =CH). ^{13}C-NMR (DMSO-d_6, 75 MHz) δ: 23.8 (C3,C5 of piperidine), 25.3 (C4 of piperidine), 44 [C2,C6 of piperidine], 55.5 (OCH_3), 76.0 (C=C–CN), 115.1 (CN), 118.7, 120.0, 121.9, 125.0, 126.1, 129.3 (aromatic carbons), 127.0 (aromatic C attached to olefinic CH), 129.4 (C of thiazolidinone attached to olefinic CH), 132.3 (aromatic C attached to N of the 4-thiazolidinone ring), 133.9 (C=CH), 159.1 (aromatic C attached to OCH_3 group), 160.2 (C=O of thiazolidinone), 164.0 (C=O), 166.0 (C=C–CN). IR (KBr) cm^{-1}: 3060–3020 (aromatic CH), 2928–2839 (aliphatic CH), 2195 (C≡N), 1713 (C=O thiazolidinone), 1636 (C=O), 1593–1508 (C=C). *Anal.* Calcd for $C_{25}H_{23}N_3O_3S$ (445.54): C, 67.40; H, 5.20; N, 9.43. Found: C, 67.30; H, 5.47; N, 9.81.

2-[5-(4-Chlorobenzylidene)-4-oxo-3-phenyl-thiazolidin-2-ylidene]-3-oxo-3-piperidin-1-yl-propionitrile (**4h**): Yellow crystals, 35% yield, mp 319–321°C (dec.). ^{1}H-NMR (DMSO-d_6, 300 MHz) δ: 1.49–1.57 (6H, m, piperidine protons), 3.43 (4H, brs, $(CH_2)_2$N piperidine protons), 7.56–7.72 (9H, m, aromatic H), 7.79 (1H, s, =CH). ^{13}C-NMR (DMSO-d_6, 100 MHz) δ: 24.0 (C3,C5 of piperidine), 25.4 (C4 of piperidine), 44.1 [C2,C6 of piperidine], 69.7 (C=C–CN), 113.1 (CN), 118.7, 120.0, 121.9, 123.5, 125.1, 126.0, 127.2 (aromatic carbons), 129.5 (C of thiazolidinone attached to olefinic CH), 131.7 (aromatic C attached to N of the 4-thiazolidinone ring), 133.7 (C=CH), 134.4 (aromatic C attached to olefinic CH), 134.7 (aromatic C attached to Cl), 153.6 (C=O of thiazolidinone), 155.0 (C=O), 166.4 (C=C–CN). IR (KBr) cm^{-1}: 3059–3028 (aromatic CH), 2928–2855 (aliphatic CH), 2195 (C≡N), 1713 (C=O thiazolidinone), 1636 (C=O), 1585–1489 (C=C). MS m/z: 449.30 (M^+), 450.30 (M^++1), 451.30 (M^++2), 338.20, 168.05, 77.10. *Anal.* Calcd for $C_{24}H_{21}ClN_3O_2S$ (449.96): C, 64.06; H, 4.48; N, 9.34. Found: C, 64.19; H, 4.71; N, 9.62.

2-[5-(2-Hydroxybenzylidene)-4-oxo-3-phenyl-thiazolidin-2-ylidene]-3-oxo-3-piperidin-1-yl-propionitrile (**4i**): Yellow crystals, 30% yield, mp 235–237°C (dec.). ^{1}H-NMR (DMSO-d_6, 300 MHz): δ 1.48–1.67 (6H, m, piperidine protons), 3.43–3.59 (4H, m, $(CH_2)_2$N piperidine protons), 6.99–8.02 (9H, m, aromatic H), 8.16 (1H, s, =CH), 10.90 (1H, s, OH

exch. D_2O). IR (KBr) cm^{-1}: 3350 (OH), 3051 (aromatic CH), 2932–2851 (aliphatic CH), 2191 (C≡N), 1701 (C=O thiazolidinone), 1636 (C=O), 1597–1493 (C=C). *Anal.* Calcd for $C_{24}H_{21}N_3O_3S$ (431.52): C, 66.80; H, 4.91; N, 9.74. Found: C, 66.90; H, 5.03; N, 9.93.

2-[5-(4-Hydroxy-3-methoxybenzylidene)-4-oxo-3-phenylthiazolidin-2-ylidene]-3-oxo-3-piperidin-1-yl-propionitrile (**4j**): Yellow crystals, 33% yield, mp 272–274°C (dec.). ^{1}H-NMR (DMSO-d_6, 300 MHz) δ: 1.49–1.57 (6H, m, piperidine protons), 3.30 (1H, brs, OH exch. D_2O), 3.44 (4H, brs, $(CH_2)_2$N piperidine protons), 3.84 (3H, s, OCH_3), 6.98–7.71 (8H, m, aromatic H), 7.79 (1H, s, =CH). ^{13}C-NMR (DMSO-d_6, 100 MHz) δ: 23.9 (C3,C5 of piperidine), 25.3 (C4 of piperidine), 44.3 [C2,C6 of piperidine], 55.9 (OCH_3), 78.3 (C=C–CN), 113.0 (CN), 116.5, 117.4, 123.8, 124.5, 126.9 (aromatic carbons), 128.8 (C of thiazolidinone attached to olefinic CH), 129.3 (aromatic C attached to olefinic CH), 133.3 (aromatic C attached to N of the 4-thiazolidinone ring), 135.1 (C=CH), 148.1 (aromatic C attached to OH), 150.2 (aromatic C attached to OCH_3), 158.8 (C=O of thiazolidinone), 162.8 (C=O), 166.2 (C=C–CN). IR (KBr) cm^{-1}: 3526 (OH), 3062–3032 (aromatic CH), 2940–2851 (aliphatic CH), 2195 (C≡N), 1717 (C=O thiazolidinone), 1663 (C=O), 1616–1516 (C=C). *Anal.* Calcd for $C_{25}H_{23}N_3O_4S$ (461.54): C, 65.06; H, 5.02; N, 9.10. Found: C, 65.18; H, 5.18; N, 9.44.

General Procedure for Preparation of Compounds (5a–h) To a mixture of **3a**, **b** (1 mmol), formaldehyde (0.10 mL, 37% in water, 1.2 mmol) in absolute ethanol (5 mL), the appropriate secondary amines (1.2 mmol) was added dropwise and the mixture was refluxed for 5 h. The precipitate obtained on cooling was filtered, washed and crystallized from ethanol/water to obtain **5a–h** in a pure form.

3-Morpholin-4-yl-3-oxo-2-(4-oxo-3-phenyl-5-pyrrolidin-1-ylmethyl-thiazolidin-2-ylidene)propionitrile (**5a**): Yellow crystals, 66% yield, mp 226–227°C (dec.). ^{1}H-NMR ($CDCl_3$, 400 MHz) δ: 1.76–1.87 (4H, m, pyrrolidine protons), 2.68–2.80 (4H, m, $(CH_2)_2$N pyrrolidine protons), 3.14–3.16 (2H, m, CH_2), 3.46–3.48 (4H, m, $(CH_2)_2$N of morpholine), 3.58–3.60 (5H, m, $(CH_2)_2$O of morpholine+CH of thiazolidinone), 7.14–7.60 (5H, m, aromatic protons). ^{13}C-NMR ($CDCl_3$, 100 MHz) δ: 24.6 [$(CH_2)_2$ pyrrolidine], 45.4 [$(CH_2)_2$N morpholine], 47.5 (C of thiazolidine attached to CH_2), 56.5 (CH_2), 56.6 [$(CH_2)_2$N pyrrolidine], 66.5 [$(CH_2)_2$O morpholine], 68.8 (C=C–CN), 113.2 (CN), 125.0, 129.7, 130.0, 131.2, 131.3 (aromatic carbons), 134.6 (aromatic C attached to N of thiazolidinone), 161.7 (C=O), 163.7 (C=O of thiazolidinone), 177.0 (C=C–CN). IR (KBr) cm^{-1}: 3067 (aromatic CH), 2967–2859 (aliphatic CH), 2203 (C≡N), 1732 (C=O thiazolidinone), 1628 (C=O), 1558–1493 (C=C). *Anal.* Calcd for $C_{21}H_{24}N_4O_3S$ (412.51): C, 61.15; H, 5.86; N, 13.58. Found: C, 61.19; H, 5.92; N, 13.74.

3-Morpholin-4-yl-3-oxo-2-(4-oxo-3-phenyl-5-piperidin-1-ylmethyl-thiazolidin-2-ylidene)propionitrile (**5b**): Yellow crystals, 45% yield, mp 214–216°C (dec.). ^{1}H-NMR ($CDCl_3$, 400 MHz) δ: 1.50–1.88 (6H, m, piperidine protons), 2.5–2.7 (4H, m, $(CH_2)_2$N of piperidine), 2.90–3.00 (2H, m, CH_2), 3.59–3.71 (8H, m, morpholine), 4.21–4.22 (1H, m, CH of thiazolidinone), 7.15–7.56 (5H, m, aromatic protons). IR (KBr) cm^{-1}: 3060 (aromatic CH), 2924–2855 (aliphatic CH), 2199 (C≡N), 1732 (C=O thiazolidinone), 1628 (C=O), 1558–1493 (C=C). *Anal.* Calcd for $C_{22}H_{26}N_4O_3S$ (426.54): C, 61.95; H, 6.14; N, 13.14. Found: C, 62.08; H, 6.22; N, 13.43.

3-Morpholin-4-yl-2-(5-morpholin-4-ylmethyl-4-oxo-3-phenyl-thiazolidin-2-ylidene)-3-oxo-propionitrile (**5c**): Orange crystals, 69% yield, mp 230–232°C (dec.). ^{1}H-NMR ($CDCl_3$, 400 MHz) δ: 2.59 (4H, brs, $(CH_2)_2$N of morpholine), 2.76 (4H, brs, $(CH_2)_2$N–CO of morpholine), 2.94–3.04 (2H, m, CH_2), 3.49–3.66 (9H, m, 8H $(CH_2)_2$O of 2 morpholine rings+CH of thiazolidinone), 7.48–7.92 (5H, m, aromatic protons). ^{13}C-NMR ($CDCl_3$, 100 MHz) δ: 46.0 [$(CH_2)_2$N morpholine], 52.1 (C of thiazolidine attached to CH_2), 55.8 [$(CH_2)_2$N morpholine], 58.3 (CH_2), 66.5 [$(CH_2)_2$O morpholine], 67.4 [$(CH_2)_2$O morpholine], 69.2 (C=C–CN), 113.3 (CN), 120.8, 123.3, 124.2, 125.8, 130.4 (aromatic carbons), 134.2 (aromatic C attached to N of thiazolidinone), 159.8 (C=O), 164.5 (C=O of thiazolidinone), 178.3 (C=C–CN). IR (KBr) cm^{-1}: 3060 (aromatic CH), 2963–2855 (aliphatic CH), 2199 (C≡N), 1732 (C=O thiazolidinone), 1628 (C=O), 1566–1493 (C=C). MS *m/z*: 428 (M^+), 341, 242, 176. *Anal.* Calcd for $C_{21}H_{24}N_4O_4S$ (428.51): C, 58.86; H, 5.65; N, 13.07. Found: C, 58.95; H, 5.71; N, 13.32.

2-[5-(4-Methylpiperazin-1-ylmethyl)-4-oxo-3-phenyl-thiazolidin-2-ylidene]-3-morpholin-4-yl-3-oxo-propionitrile (**5d**): Yellow crystals, 43% yield, mp 222–224°C (dec.). ^{1}H-NMR ($CDCl_3$, 400 MHz) δ: 1.86 (3H, s, CH_3), 2.25 (4H, brs, $(CH_2)_2$N piperazine), 2.70 (4H, brs, $(CH_2)_2$N piperazine), 3.00 (2H, brs, CH_2), 3.50–3.61 (9H, m, 4H $(CH_2)_2$N morpholine + 4H $(CH_2)_2$O morpholine+CH of thiazolidinone), 7.38–7.72 (5H, m, aromatic protons). IR (KBr) cm^{-1}: 3060 (aromatic CH), 2963–2801 (aliphatic CH), 2199 (C≡N), 1732 (C=O thiazolidinone), 1628 (C=O), 1558–1493 (C=C). *Anal.* Calcd for $C_{22}H_{27}N_5O_3S$ (441.56): C, 59.84; H, 6.16; N, 15.86. Found: C, 59.93; H, 6.30; N, 16.12.

3-Oxo-2-(4-oxo-3-phenyl-5-pyrrolidin-1-ylmethyl-thiazolidin-2-ylidene)-3-piperidin-1-yl-propionitrile (**5e**): Yellow crystals, 46% yield, mp 184–186°C (dec.). ^{1}H-NMR ($CDCl_3$, 400 MHz) δ: 1.63–1.85 (10H, m, 4H pyrrolidine protons+6H piperidine protons), 2.68–2.87 (4H, m, $(CH_2)_2$N pyrrolidine protons), 3.14–3.16 (2H, m, CH_2), 3.42–3.55 (4H, m, $(CH_2)_2$N of piperidine), 3.68–3.80 (1H, m, CH of thiazolidinone), 7.16–7.55 (5H, m, aromatic protons). IR (KBr) cm^{-1}: 3060 (aromatic CH), 2936–2808 (aliphatic CH), 2199 (C≡N), 1732 (C=O thiazolidinone), 1628 (C=O), 1558–1493 (C=C). *Anal.* Calcd for $C_{22}H_{26}N_4O_2S$ (410.54): C, 64.36; H, 6.38; N, 13.65. Found: C, 64.47; H, 6.41; N, 13.78.

3-Oxo-2-(4-oxo-3-phenyl-5-piperidin-1-ylmethyl-thiazolidin-2-ylidene)-3-piperidin-1-yl-propionitrile (**5f**): Yellow crystals, 46% yield, mp 183–185°C (dec.). ^{1}H-NMR ($CDCl_3$, 400 MHz) δ: 1.25–1.57 (12H, m, two piperidine rings protons), 2.49–2.67 (4H, m, $(CH_2)_2$N of piperidine), 2.90–3.00 (2H, m, CH_2), 3.45–3.56 (4H, m, $(CH_2)_2$N of piperidine), 4.20–4.22 (1H, m, CH of thiazolidinone), 7.16–7.53 (5H, m, aromatic protons). ^{13}C-NMR ($CDCl_3$, 100 MHz) δ: 24.6 (C3,C5 of piperidine), 25.3 (C4 of piperidine), 25.8 (C3,C4,C5 of piperidine), 40.5 [C2,C6 piperidine], 51.2 (C of thiazolidinone attached to CH_2), 51.5 [C2,C6 piperidine], 57.0 (CH_2), 70.7 (C=C–CN), 114.2 (CN), 120.0, 123.3, 124.4, 128.9, 129.4 (aromatic carbons), 133.3 (aromatic C attached to N of thiazolidinone), 158.0 (C=O), 164.0 (C=O of thiazolidinone), 178.8 (C=C–CN); IR (KBr) cm^{-1}: 3050 (aromatic CH), 2936–2855 (aliphatic CH), 2199 (C≡N), 1728 (C=O thiazolidinone), 1628 (C=O), 1570–1493 (C=C). *Anal.* Calcd for $C_{23}H_{28}N_4O_2S$ (424.57): C, 65.07; H, 6.65; N, 13.20. Found: C, 65.14; H, 6.73; N, 13.51.

2-(5-Morpholin-4-ylmethyl-4-oxo-3-phenyl-thiazolidin-

2-ylidene)-3-oxo-3-piperidin-1-yl-propionitrile (**5g**): Orange crystals, 50% yield, mp 224–226°C (dec.). ^{1}H-NMR ($CDCl_3$, 400 MHz) δ: 1.28–1.49 (6H, m, piperidine protons), 2.57–2.74 (4H, m, $(CH_2)_2N$ of morpholine), 2.85–2.95 (2H, m, CH_2), 3.38–3.40 (4H, m, $(CH_2)_2N$ of piperidine), 3.65–3.68 (5H, m, $(CH_2)_2O$ of morpholine+CH of thiazolidinone), 7.35–7.75 (5H, m, aromatic protons). IR (KBr) cm^{-1}: 3050 (aromatic CH), 2940–2855 (aliphatic CH), 2199 (C≡N), 1732 (C=O thiazolidinone), 1624 (C=O), 1570–1493 (C=C). *Anal.* Calcd for $C_{22}H_{26}N_4O_3S$ (426.54): C, 61.95; H, 6.14; N, 13.14. Found: C, 62.04; H, 6.12; N, 13.39.

2-[5-(4-Methylpiperazin-1-ylmethyl)-4-oxo-3-phenyl-thiazolidin-2-ylidene]-3-oxo-3-piperidin-1-yl-propionitrile (**5h**): Off white crystals, 46% yield, mp 198–200°C (dec.). ^{1}H-NMR ($CDCl_3$, 400 MHz) δ: 1.45–1.65 (6H, m, piperidine protons), 1.95 (3H, s, CH_3), 2.25–2.30 (4H, m, $(CH_2)_2N$ of piperazine), 2.60–2.65 (4H, m, $(CH_2)_2N$ of piperazine), 2.90–3.10 (2H, m, CH_2), 3.40–3.47 (4H, m, $(CH_2)_2N$ of piperidine), 3.75–3.77 (1H, m, CH of thiazolidinone), 7.33–7.76 (5H, m, aromatic protons). ^{13}C-NMR ($CDCl_3$, 100 MHz) δ: 24.5 (2C of piperidine), 25.7 (C of piperidine), 43.3 (CH_3), 45.8 [$(CH_2)_2N$ piperidine], 48.5 (C of thiazolidinone attached to CH_2), 52.1 [$(CH_2)_2N$ piprazine], 56.3 [$(CH_2)_2N$ piprazine], 59.2 (CH_2), 69.2 (C=C–CN), 113.8 (CN), 120.0, 125.0, 128.9, 129.0, 129.9 (aromatic carbons), 135.0 (aromatic C attached to N of thiazolidinone), 157.1 (C=O), 163.3 (C=O of thiazolidinone), 177.9 (C=C–CN). IR (KBr) cm^{-1}: 3050 (aromatic CH), 2940–2801 (aliphatic CH), 2199 (C≡N), 1732 (C=O thiazolidinone), 1628 (C=O), 1570–1493 (C=C). MS *m/z*: 439.30 (M^+), 327, 211, 177. *Anal.* Calcd for $C_{23}H_{29}N_5O_2S$ (439.58): C, 62.84; H, 6.65; N, 15.93. Found: C, 62.78; H, 6.70; N, 16.18.

General Procedure for the Preparation of (6a, b) A solution of **2a**, **b** (6 mmol) and TEA (1.22 g, 1.65 mL, 12 mmol) in dry THF (15 mL) was cooled to −5°C in an ice/salt bath and a solution of 3-chloroapropionyl chloride (0.76 g, 0.60 mL, 6 mmol) in dry THF (10 mL) was added dropwise. The mixture was stirred overnight at room temperature, and the formed precipitate was filtered and dried. The residue was suspended in water, stirred for 5 min, and filtered. The crude product was crystallized from ethanol.

(2*E*) 3-Morpholin-4-yl-3-oxo-2-(4-oxo-3-phenyl-[1,3]-thiazinan-2-ylidene)-propionitrile (**6a**): White crystals, 71% yield, mp 196–198°C. ^{1}H-NMR ($CDCl_3$) δ: 2.95–3.06 (m, 2H, $CO\underline{CH_2}CH_2S$), 3.14–3.16 (m, 2H, $COCH_2\underline{CH_2}S$), 3.27–3.29 (m, 4H, morpholinyl $(CH_2)_2$ N), 3.35–3.40 (m, 4H, morpholinyl $(CH_2)_2$ O), 7.21–7.50 (m, 5H, aromatic protons). IR (KBr) cm^{-1}: 3040 (aromatic CH), 2982–2862 (aliphatic CH), 2199 (C≡N), 1713 (C=O thiazinanone), 1643 (C=O), 1531–1490 (C=C). *Anal.* Calcd for $C_{17}H_{17}N_3O_3S$ (343.41): C, 59.46; H, 4.99; N, 12.24. Found: C, 59.06; H, 5.29; N, 12.39.

(2*E*) 3-Oxo-2-(4-oxo-3-phenyl-[1,3]thiazinan-2-ylidene)-3-piperidin-1-yl-propionitrile (**6b**): White crystals, 70% yield, mp 211–213°C. ^{1}H-NMR ($CDCl_3$) δ: 1.68 (6H, m, piperidinyl protons), 3.12–3.15 (6H, m, 4H piperidinyl$(CH_2)_2$N+2H $CO\underline{CH_2}CH_2S$), 3.26–3.28 (2H, m, $COCH_2\underline{CH_2}S$), 7.20–7.50 (5H, m, aromatic protons). IR (KBr) cm^{-1}: 3059 (aromatic CH), 2924–2859 (aliphatic CH), 2195 (C≡N), 1709 (C=O thiazinanone), 1620 (C=O), 1524–1493 (C=C). *Anal.* Calcd for $C_{18}H_{19}N_3O_2S$ (341.44): C, 63.32; H, 5.61; N, 12.31. Found: C, 63.41; H, 5.63; N, 12.56.

Single Crystal X-Ray Crystallographic Data of (6a)[42] For X-ray crystallographic studies, compound **6a** was recrystallized as prismatic colourless crystals from ethanol. The crystallographic data were collected at T=298 K on a Kappa CCD Enraf Nonius FR 590 diffractometer using a graphite monochromator with Mo-$K\alpha$ radiation (λ=0.71073 Å). The crystal structures were determined by SIR92[43] and refined by maXus[44] (Bruker Nonius, Delft and MacScience, Japan). Chemical formula $C_{17}H_{17}N_3O_3S$, M_r=343.405, monoclinic, crystallizes in space group $P2_1/c$, cell lengths "a=8.2306 (2), b=17.5581 (4), c=12.8758 (4) Å," cell angles "α=90.00°, β=12 (18)×10^1°, γ=90.00°," V=1617.86 (13) Å^3, Z=4, D_c=1.392 mg/m^3, θ values 2.910–27.485°, absorption coefficient μ (Mo-$K\alpha$)= 0.22 mm^{-1}, F(000)=720. The unique reflections measured 4148 of which 2406 reflections with threshold expression $I>3\sigma(I)$ were used in the structural analysis. Convergence for 217 variable parameters by least-squares refinement on F^2 with $w=1/[\sigma^2(F_o^2)+0.10000F_o^2]$. The final agreement factors were R=0.044 and wR=0.175 with a goodness-of-fit of 1.119.

Antitumor Activity The potential cytotoxicity of the tested compounds was evaluated using the method of Skehan *et al.*[15,29–35] Cells were plated in 96-multiwell plate (10^4 cells/well) for 24 h before treatment with the prepared compounds to allow the attachment of cells to the wall of the plate. The tested compounds were dissolved in dimethylsulfoxide (DMSO) and diluted 1000-fold in the assay. Concentrations 0, 5, 12.5, 25, and 50 μg/mL of the tested compounds were added to the cell monolayer. The monolayer cells were incubated with the compounds for 48 h at 37°C, in atmosphere of 5% CO_2. After 48 h, the cells were fixed, washed and stained with Sulfo-Rhodamine-B stain (SRB). Excess stain was washed with acetic acid. The attached stain was recovered with Tris EDTA buffer. Cell survival and drug activity were determined by measuring color intensity using an enzyme-linked immunosorbent assay (ELISA) reader. Data are representative of the individual experiment, performed in three replicates for each individual dose and measured by SRB assay. Control values did not exhibit significant changes compared to the DMSO vehicle. The IC_{50} was determined by using a program Graph-Pad PRISM version 5. Mean and standard error were determined by SPSS 11 software.

Acknowledgement The authors are thankful to Dr. Nasser S. M. Ismail, Pharmaceutical Chemistry Department, Faculty of Pharmacy, Ain Shams University, for his assistance in performing the QSAR study.

References

1) American Cancer Society, Atlanta, "Cancer Facts & Figures." ‹http://www.cancer.org/acs/groups/content/@epidemiologysurveilance/documents/document/acspc-031941.pdf›, 2012.
2) Smith R. A., Cokkinides V., Brawley O. W., *CA Cancer J. Clin.*, **59**, 27–41 (2009).
3) Lesyk R., Vladzimirska O., Holota S., Zaprutko L., Gzella A., *Eur. J. Med. Chem.*, **42**, 641–648 (2007).
4) Xia Z., Knaak C., Ma J., Beharry Z. M., McInnes C., Wang W., Kraft A. S., Smith C. D., *J. Med. Chem.*, **52**, 74–86 (2009).
5) Havrylyuk D., Zimenkovsky B., Vasylenko O., Zaprutko L., Gzella A., Lesyk R., *Eur. J. Med. Chem.*, **44**, 1396–1404 (2009).
6) Kaminskyy D., Zimenkovsky B., Lesyk R., *Eur. J. Med. Chem.*, **44**, 3627–3636 (2009).
7) Lu Y., Wang Z., Li C.-M., Chen J., Dalton J. T., Li W., Miller D. D., *Bioorg. Med. Chem.*, **18**, 477–495 (2010).

8) Havrylyuk D., Mosula L., Zimenkovsky B., Vasylenko O., Gzella A., Lesyk R., *Eur. J. Med. Chem.*, **45**, 5012–5021 (2010).
9) Subtel'na I., Atamanyuk D., Szymańska E., Kieć-Kononowicz K., Zimenkovsky B., Vasylenko O., Gzella A., Lesyk R., *Bioorg. Med. Chem.*, **18**, 5090–5102 (2010).
10) Patil V., Tilekar K., Mehendale-Munj S., Mohan R., Ramaa C. S., *Eur. J. Med. Chem.*, **45**, 4539–4544 (2010).
11) Li Q., Wu J., Zheng H., Liu K., Guo T. L., Liu Y., Eblen S. T., Grant S., Zhang S., *Bioorg. Med. Chem. Lett.*, **20**, 4526–4530 (2010).
12) Kamel M. M., Ali H. I., Anwar M. M., Mohamed N. A., Soliman A. M., *Eur. J. Med. Chem.*, **45**, 572–580 (2010).
13) Salamone S., Colin C., Grillier-Vuissoz I., Kuntz S., Mazerbourg S., Flament S., Martin H., Richert L., Chapleur Y., Boisbrun M., *Eur. J. Med. Chem.*, **51**, 206–215 (2012).
14) Liu K., Rao W., Parikh H., Li Q., Guo T. L., Grant S., Kellogg G. E., Zhang S., *Eur. J. Med. Chem.*, **47**, 125–137 (2012).
15) George R. F., *Eur. J. Med. Chem.*, **47**, 377–386 (2012).
16) Menear K. A., Gomez S., Malagu K., Bailey C., Blackburn K., Cockcroft X.-L., Ewen S., Fundo A., Le Gall A., Hermann G., Sebastian L., Sunose M., Presnot T., Torode E., Hickson I., Martin N. M. B., Smith G. C. M., Pike K. G., *Bioorg. Med. Chem. Lett.*, **19**, 5898–5901 (2009).
17) Lin H., Erhard K., Hardwicke M. A., Luengo J. I., Mack J. F., McSurdy-Freed J., Plant R., Raha K., Rominger C. M., Sanchez R. M., Schaber M. D., Schulz M. J., Spengler M. D., Tedesco R., Xie R., Zeng J. J., Rivero R. A., *Bioorg. Med. Chem. Lett.*, **22**, 2230–2234 (2012).
18) Wang J., Wang X., Chen Y., Chen S., Chen G., Tong L., Meng L., Xie Y., Ding J., Yang C., *Bioorg. Med. Chem. Lett.*, **22**, 339–342 (2012).
19) Li S., Lei Y., Jia Y., Li N., Wink M., Ma Y., *Phytomedicine*, **19**, 83–87 (2011).
20) Rossi C., Porcelloni M., D'Andrea P., Fincham C. I., Ettorre A., Mauro S., Squarcia A., Bigioni M., Parlani M., Nardelli F., Binaschi M., Maggi C. A., Fattori D., *Bioorg. Med. Chem. Lett.*, **21**, 2305–2308 (2011).
21) Ranise A., Schenone S., Bruno O., Bondavalli F., Filippelli W., Falcone G., Rivaldi B., *Il Farmaco*, **56**, 647–657 (2001).
22) Whitehead C. W., Traverso J. J., *J. Am. Chem. Soc.*, **77**, 5867–5872 (1955).
23) Bruno G., Costantino L., Curinga C., Maccari R., Monforte F., Nicoló F., Ottanà R., Vigorita M. G., *Bioorg. Med. Chem.*, **10**, 1077–1084 (2002).
24) Ottanà R., Maccari R., Barreca M. L., Bruno G., Rotondo A., Rossi A., Chiricosta G., Di Paola R., Sautebin L., Cuzzocrea S., Vigorita M. G., *Bioorg. Med. Chem.*, **13**, 4243–4252 (2005).
25) Vicini P., Geronikaki A., Anastasia K., Incerti M., Zani F., *Bioorg. Med. Chem.*, **14**, 3859–3864 (2006).
26) Gabillet S., Lecerclé D., Loreau O., Carboni M., Dézard S., Gomis J. M., Taran F., *Org. Lett.*, **9**, 3925–3927 (2007).
27) Erol S., Dogan I., *J. Org. Chem.*, **72**, 2494–2500 (2007).
28) Abdel-Aziz H. A., El-Zahabi H. S. A., Dawood K. M., *Eur. J. Med. Chem.*, **45**, 2427–2432 (2010).
29) Skehan P., Storeng R., Scudiero D., Monks A., McMahon J., Vistica D., Warren J. T., Bokesch H., Kenney S., Boyd M. R., *J. Natl. Cancer Inst.*, **82**, 1107–1112 (1990).
30) Alley M. C., Scudiero D. A., Monks A., Hursey M. L., Czerwinski M. J., Fine D. L., Abbott B. J., Mayo J. G., Shoemaker R. H., Boyd M. R., *Cancer Res.*, **48**, 589–601 (1988).
31) Grever M. R., Schepartz S. A., Chabner B. A., *Semin. Oncol.*, **19**, 622–638 (1992).
32) Boyd M. R., Paull K. D., *Drug Dev. Res.*, **34**, 91–109 (1995).
33) Girgis A. S., Hosni H. M., Barsoum F. F., *Bioorg. Med. Chem.*, **14**, 4466–4476 (2006).
34) Katritzky A. R., Girgis A. S., Slavov S., Tala S. R., Stoyanova-Slavova I., *Eur. J. Med. Chem.*, **45**, 5183–5199 (2010).
35) Girgis A. S., Stawinski J., Ismail N. S. M., Farag H., *Eur. J. Med. Chem.*, **47**, 312–322 (2012).
36) Taha M. O., Bustanji Y., Al-Ghussein M. A. S., Mohammad M., Zalloum H., Al-Masri I. M., Atallah N., *J. Med. Chem.*, **51**, 2062–2077 (2008).
37) Taha M. O., Bustanji Y., Al-Bakri A. G., Yousef A. M., Zalloum W. A., Al-Masri I. M., Atallah N., *J. Mol. Graph. Model.*, **25**, 870–884 (2007).
38) Abu Khalaf R., Abu Sheikha G., Bustanji Y., Taha M. O., *Eur. J. Med. Chem.*, **45**, 1598–1617 (2010).
39) Al-Masri I. M., Mohammad M. K., Taha M. O., *ChemMedChem*, **3**, 1763–1779 (2008).
40) Duchowicz P. R., Vitale M. G., Castro E. A., Autino J. C., Romanelli G. P., Bennardi D. O., *Eur. J. Med. Chem.*, **43**, 1593–1602 (2008).
41) Abdel-Aziz H. A., Abdel-Wahab B. F., El-Sharief M. A. M. Sh., Abdulla M. M., *Monatsh. Chem.*, **140**, 431–437 (2009).
42) Full crystallographic details, excluding structure factors, have been deposited at Cambridge Crystallographic Data Center (CCDC) as supplementary publication number CCDC 889159.
43) Altomare A., Cascarano G., Giacovazzo C., Guagliardi A., Burla M. C., Polidori G., Camalli M., *J. Appl. Cryst.*, **27**, 435–436 (1994).
44) Mackay S., Gilmore C. J., Edwards C., Stewart N., Shankland K., "maXus Computer Program for the Solution and Refinement of Crystal Structures," Bruker Nonius, the Netherlands, MacScience, Japan, and The University of Glasgow, the Netherlands, 1999.